ISSN 0965-5425, Computational Mathematics and Mathematical Physics, 2025, Vol. 65, No. 5, pp. 949–965. © Pleiades Publishing, Ltd., 2025.

PARTIAL DIFFERENTIAL EQUATIONS

On the Propagation Direction of Traveling Waves

V. V. Vedeneev*

Steklov Mathematical Institute of the Russian Academy of Sciences, Moscow, 119333 Russia

**e-mail: vasily@vedeneev.ru*

Received October 27, 2024; revised November 1, 2024; accepted February 25, 2025

Abstract—In a number of problems related to the spatial propagation of waves, it is necessary to distinguish between waves moving in one and in the other direction. Examples of such problems include the propagation of waves from a point pulsating source, the problem of spatial optimal disturbances, the problem of determining the absolute or convective nature of instability, etc. In addition, when calculating wave motion in an inhomogeneous medium by marching methods, the solution is projected onto the subspace of waves propagating in one direction for numerical stabilization, which also requires their correct filtering. In the literature, the generally accepted indicators of the direction of wave propagation are the Briggs criterion, which follows from the causality principle, and, in some works, the sign of the group velocity. This paper discusses their interpretations and the relationship between them. Examples are given in which the identification of the wave propagation direction by the sign of the group velocity is erroneous and leads to qualitatively incorrect results. For the first time, a case is considered where the direct application of the Briggs criterion is impossible due to the absorption of the discrete mode representing the wave by the continuous spectrum. A generalization of the Briggs criterion for this case is given and examples of its application are discussed.

Keywords: traveling wave, phase velocity, group velocity, Briggs criterion, continuous spectrum

DOI: 10.1134/S0965542525700277

1. INTRODUCTION

In the one-dimensional wave theory, i.e., in the theory of solutions $\sim e^{i(kx-\omega t)}$ to the linearized equations, important issue is to determine the direction in which a particular wave propagates. For example, when solving a problem about a harmonically oscillating source located at the point $x = 0$ on a uniform background for a system in which for each frequency ω there are N solutions $k_n(\omega)$ to the dispersion equation, the solution on one side and on the other side of the source is

$$\sum_n A_n e^{i(k_n(\omega)x-\omega t)}, \tag{1.1}$$

where the sum to the left of the source is taken only over the waves travelling to the left and the sum to the right of the source is taken only over the waves travelling to the right.

If the system under consideration is semi-infinite, i.e., if it is defined for $x \geqslant 0$, then the waves moving to the left cannot propagate in such a system; in other words, in the general solution (1.1) it is also necessary to keep only the waves moving away from the boundary, and the number of boundary conditions posed on this boundary must be equal to the number of waves moving away from it [1].

Similarly, in problems of optimal spatial disturbances in semi-infinite systems defined for $x \geqslant 0$, such as boundary layers [2], flow in a pipe [3], submerged jets [4–6], etc., for the mathematical well-posedness and physical adequacy of the problem, it is necessary to leave in expansion (1.1) only waves moving to the right.

In studying the propagation of disturbances over an inhomogeneous background, e.g., the development of a Tollmien–Schlichting wave in a boundary layer growing on a body, parabolized Navier–Stokes equations are used ([7], Subsection 7.4.3), which are also associated with distinguishing the waves propagating downstream. A more recent concept eliminating the known numerical problems of parabolized equations, is to construct one-way Navier–Stokes equations, in which case the waves moving over the flow are "removed" from the system [8, 9]. A somewhat different approach called spectral reduction was used in [10]: the disturbance at each spatial step when moving downstream was projected onto the sub-

space of eigenmodes corresponding to the waves moving downstream. In this case, it is extremely important to physically justify the selection of modes included in this subspace. A comparison of various approaches to calculating disturbances developing in space can be found in [11].

Another example of problems in which it is important to identify the direction of wave motion is the problem of absolute and convective instability. Its solution is reduced to finding saddle points of the function $\omega(k)$, or, equivalently, of the branching points of the inverse function $k(\omega)$. In this case, only the points at which there is branching of the wave numbers corresponding to the waves moving in the opposite directions contribute to the asymptotics of disturbances ([12], Subsection 7.4).

Thus, in a number of problems it is required to separate the spectrum of spatial waves $e^{i(k_n x-\omega t)}$, $n = 1,\ldots,N$, into waves moving to the right and waves moving to the left. However, the question of the method of such a separation is far from obvious. In the general case, the complex frequency and wave number are related by the dispersion relation

$$F(k,\omega) = 0, \tag{1.2}$$

which can have a very complex structure; as a consequence, its roots $k_n(\omega)$ can have branching points and cuts, so that one "wave" transforms into another "wave" with a continuous change in frequency and transition to another sheet of the Riemann surface. In this regard, the very concept of a separate "wave" must be specified by identifying single-valued sheets of the Riemann surface. Moreover, relation (1.2) may not have an algebraic form; e.g., in problems of hydrodynamic stability, the spectrum $k_n(\omega)$ may have a countable or continuous subset. Therefore, it is important to have a universal indicator of the direction of wave propagation independent of the specific nature of the problem.

For definiteness, below by a separate spatial "wave" or "mode" we mean a single-valued function $k_n(\omega)$ defined on the entire complex plane ω except, maybe, for isolated singularities and cuts, as well as the motion described by it, which has the form $e^{i(k_n(\omega)x-\omega t)}$. Let us formulate what will be understood below by the "direction of wave motion." Let an external disturbance in the form of a source localized in space and harmonic in time be introduced into a system at rest at the time $t = 0$. Then disturbances in the form of a linear combination of waves will start to propagate to the right and left of the source. The waves that appear in the solution to the problem to the right of the source will be called propagating to the right, and the waves that appear in the solution to the left of the source will be called propagating to the left. Note that the direction of wave motion in a physically adequate and mathematically well-posed problem should not depend on frequency, i.e. it is a property of the wave as a whole.

Below, in Section 2, we consider the well-known "naïve" approaches to identifying the direction of wave motion—phase and group velocity—and demonstrate their inconsistency. In Section 3, we take as a basis a physically justified method for identifying the direction of waves—the causality principle—which leads to the so-called Briggs criterion for the direction of wave motion. We analyze its relationship with the naive direction indicators. Using the example of a problem of wind waves on water, which admits an analytical solution, we discuss the situation when the Briggs criterion does not coincide with any of the naïve indicators, and also study the situation when the causality principle cannot be straightforwardly applied due to the "disappearance" of some modes when the frequency changes. A generalization of the Briggs criterion for this case is derived. In Section 4, we consider the problem of hydrodynamic stability of a submerged jet, in which both "counterintuitive" wave behaviors are present—incorrect indication of the direction of wave propagation by the phase and group velocity and vanishing modes. Section 5 briefly formulates the results of the work.

2. NAÏVE INDICATORS OF THE TRAVELING WAVE PROPAGATION DIRECTION

2.1. Phase Velocity

The simplest characteristic of a traveling wave $e^{i(kx-\omega t)}$ specified by the wave number k and frequency ω (which are, in general, complex) is its phase velocity $c = \omega/k$. If the wave number k is real, then $\operatorname{Re} c$ coincides with the velocity of the wave "crests" motion, and $\operatorname{Im} c$ is responsible for the amplification and attenuation of the wave amplitude. At first glance, it is natural to take the sign of $\operatorname{Re} c$, i.e., the direction of motion of the wave crests and troughs, as a criterion for the direction of its motion as a whole.

However, it is easy to understand that such a criterion is not universal. Let us consider as an example a model of wind over a fluid surface: a layer of ideal incompressible fluid of infinite depth over which a lighter ideal incompressible fluid moves (Fig. 1). The effect of gravity and the surface tension of the inter-

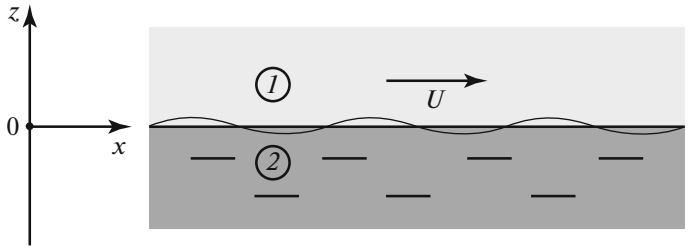

Fig. 1. Waves on the surface of heavy fluid with a lighter fluid moving above it.

face are taken into account. The dispersion equation describing the waves at the interface of two media is written as (see [13], Chapter 8, Section 13)

$$\rho_1(\omega - Uk)^2 + \rho_2\omega^2 = (\rho_2 - \rho_1)g|k| + N|k|^3,$$

where ρ_i are the media densities, U is the wind velocity, g is acceleration of gravity, and N is the surface tension coefficient. By choosing ρ_1, g, and N as dimensionally independent scales, we rewrite this equation in dimensionless form used in the subsequent analysis as

$$(\omega - Uk)^2 + \varkappa\omega^2 = (\varkappa - 1)|k| + |k|^3, \tag{2.1}$$

where $\varkappa = \rho_2/\rho_1 > 1$ and the notation of the other dimensionless variables is the same.

The dispersion equation (2.1) is obtained for real values of k; however, it can be analytically continued to the entire complex plane of k if the modulus sign is understood as follows:

$$|k| = \begin{cases} k & \text{if} \quad \operatorname{Re} k \geqslant 0, \\ -k & \text{if} \quad \operatorname{Re} k < 0. \end{cases}$$

This continuation is dictated by the condition of attenuation of disturbances with distance from the boundary of the interface, i.e., as $|z| \to \infty$. The line $\operatorname{Re} k = 0$ is a cut of the complex plane of the values of k. This is how the modulus symbol will be understood below when considering the complex values of k.

Consider the temporal stability problem, i.e., find solutions $\omega(k)$ to Eq. (2.1) or, equivalently, $c(k)$:

$$c_\pm(k) = \frac{\omega}{k} = \frac{1}{\varkappa + 1}\left(U \pm \sqrt{U^2 + (\varkappa + 1)\left(\frac{\varkappa - 1}{|k|} + |k| - U^2\right)}\right). \tag{2.2}$$

For each wave number k, there are two waves with phase velocities $c(k)$. If the radicand is positive at $k \in \mathbb{R}$, then both waves are neutrally stable; otherwise, for one of the waves $\operatorname{Im} c(k) > 0$, i.e., there is a wave number $k \in \mathbb{R}$ such that $\operatorname{Im}\omega > 0$; such a wave is growing. Instability, i.e., the presence of growing waves, occurs for $U > U_{\mathrm{cr}}$, where

$$U_{\mathrm{cr}} = \sqrt{\frac{\varkappa + 1}{\varkappa}\min_k\left(\frac{\varkappa - 1}{|k|} + |k|\right)} = \sqrt{2\frac{\varkappa + 1}{\varkappa}\sqrt[4]{\varkappa - 1}}. \tag{2.3}$$

Below, we consider only the case $U < U_{\mathrm{cr}}$ when the system under examination is stable. It is easy to see that the phase velocity of one of the waves is always directed to the right, i.e., $c_+(k) > 0$—it corresponds to the plus sign in (2.2). However, the direction of the phase velocity of the other wave depends on the wind velocity U. More precisely, if $U < U_{\mathrm{c0}}$, then it is directed to the left, i.e., $c_-(k) < 0$; however, for $U_{\mathrm{c0}} < U < U_{\mathrm{cr}}$, where

$$U_{\mathrm{c0}} = U_{\mathrm{cr}}\left(1 + \frac{1}{\varkappa}\right)^{-1/2},$$

there is a range of k such that $c_-(k) > 0$. This range of k includes the value $k = \sqrt{\varkappa - 1}$ at which (2.3) has a minimum. An example of the dependence $c(k)$ is shown in Fig. 2a for the parameters

$$\varkappa = 10, \quad U = 2.5. \tag{2.4}$$

This value of $\varkappa$ corresponds to $U_{c0} \approx 2.449$, $U_{cr} \approx 2.569$.

Thus, with a continuous change in wind velocity, the crests of a wave moving to the left turn and begin to move to the right. Consequently, the direction of motion of the wave crests, i.e. sign $\operatorname{Re} c$, is inconsistent for identifying the direction of motion of the wave as a whole in the sense defined in Section 1.

2.2. Group Velocity

The group velocity is defined as

$$g(k) = \frac{d\omega(k)}{dk},$$

and it describes the velocity of motion of the localized wave packet (group of waves) ([14], Section 67). Since localized sources may be considered as separate "signals", the group velocity is usually interpreted as the rate of information transfer in the system. Usually, $g(k) \neq c(k)$ due to the dispersion of waves in the general case; moreover, the group and phase velocities can, generally speaking, have opposite signs.

In the literature, it is the sign of the group velocity that is often considered as an indicator of the wave propagation direction ([7], Subsection 7.1). At first glance, this seems logical—the motion of the pulse signal should be related to the motion of the wave as a whole. However, the group velocity, just like the phase velocity, can change direction with a continuous change in frequency or problem parameters. Namely, in the example considered above, the group velocity is calculated explicitly using (2.2) as $g(k) = d(c(k)k)/dk$. From the qualitative shape of the graph $c(k)$, one can construct a qualitative shape of the graph of $g(k)$, from which the change in the direction of the group velocity at the velocity $U_{g0} < U_{c0}$ is obvious. An example is shown in Fig. 2b for parameters (2.4); in this case, $U_{g0} \approx 2.115$.

Below, we show that the identification of the direction of wave propagation by the group velocity is correct only for the analysis of the fastest growing wave; however, in the general case it may be erroneous.

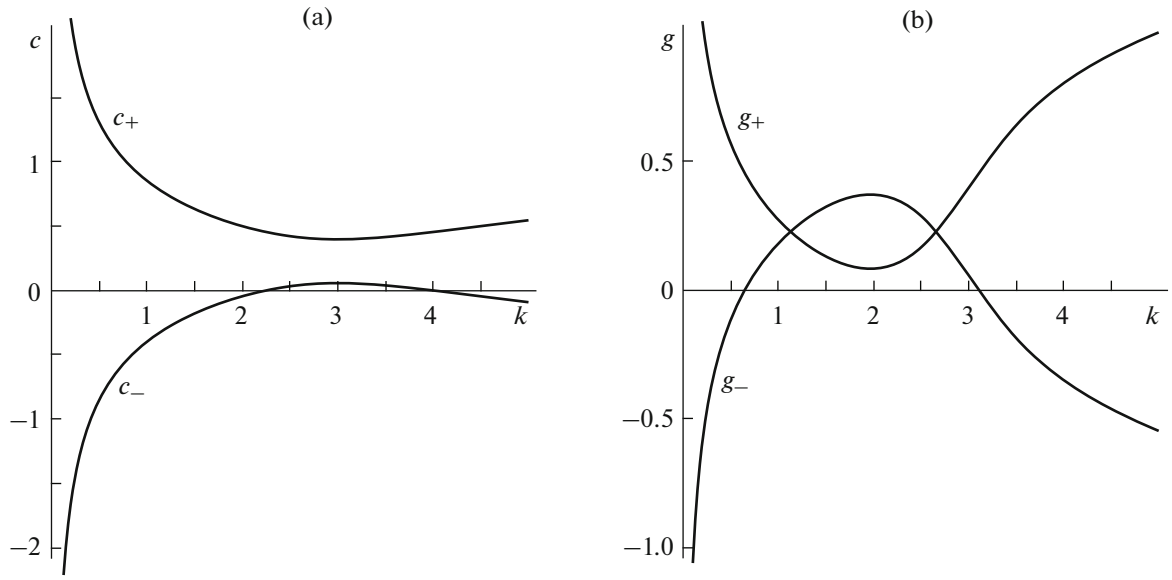

Fig. 2. Dependence of the phase (a) and group (b) velocity on the real wave number for the dispersion equation (2.1).

3. CAUSALITY PRINCIPLE AND THE BRIGGS CRITERION

Let us formulate the causality principle, which any correct linear mathematical model describing the behavior of small disturbances in real physical processes must satisfy: no disturbance of a physical system can grow infinitely fast in a finite time. In other words, a disturbance in a certain region of space cannot cause infinite growth in this or any other region of space. If such growth takes place, it must be caused by

some other reasons, e.g., by waves coming from infinity. From the point of view of an adequate mathematical formulation of a physical problem, there should be no solutions whose cause is not the disturbance introduced into the system, i.e., incoming waves must be excluded.

For example, in problems of acoustic wave emission described by the wave equation, the "Sommerfeld radiation condition" is usually set—the selection at infinity of one of the two waves—the one leaving from the place where the disturbance originates, i.e., the one whose group velocity is directed away from the source. It can be shown that this condition *for the wave equation* is a special case of the general Briggs criterion for determining the direction of wave propagation.

For systems satisfying the principle of causality, the corresponding mathematical problem is inevitably well-posed according to Petrovskii [15]. Namely, since disturbances cannot grow indefinitely fast, there must be a maximum increment of traveling waves $M = \max_{k\in\mathbb{R}} \operatorname{Im}\omega(k) < \infty$, where $\omega(k)$ are solutions of the dispersion equation. Otherwise, there would be disturbances growing infinitely fast, i.e., the system would "explode". Examples of problems that do not satisfy the well-posedness condition are well known; e.g., this is a tangential discontinuity between two incompressible fluids, in which the growth of short waves is unbounded, but which is suppressed when taking into account the surface tension of the interface.

It turns out that the natural causality requirement is sufficient for obtaining a physically justified criterion of the direction of wave propagation ([16], Subsection 2.3).

3.1. Solution to the Cauchy Problem and the Briggs Criterion

Without specifying the physical system under examination for the time being, let us consider the source problem: let there be an external disturbance in some localized region of space acting according to a harmonic law with frequency $\omega_0 \in \mathbb{R}$. We will solve the Cauchy problem that will allow us to determine the components of the disturbances that run out from the source to the left and to the right. Below, we describe the scheme for solving this problem that basically corresponds to [16], Subsection 2.3, and [17].

Suppose we have n variables $u_1(x,t)$, ..., $u_n(x,t)$ that describe the system state, and let the linearized system of equations for disturbances have the general form

$$P_{11}u_1 + P_{12}u_2 + \ldots + P_{1n}u_n = f_1\delta(x)e^{-i\omega_0 t}H(t),$$

$$P_{21}u_1 + P_{22}u_2 + \ldots + P_{2n}u_n = f_2\delta(x)e^{-i\omega_0 t}H(t),$$

$$\ldots\ldots\ldots\ldots$$

$$P_{n1}u_1 + P_{n2}u_2 + \ldots + P_{nn}u_n = f_n\delta(x)e^{-i\omega_0 t}H(t),$$

where $P_{ij} = P_{ij}\left(\frac{\partial}{\partial x}, \frac{\partial}{\partial t}\right)$ are polynomials of $\partial/\partial x$ and $\partial/\partial t$, f_i are amplitudes of the external force, $\delta(x)$ is the delta function, and $H(t)$ is the Heaviside function. This system may also include other directional derivatives; e.g., in the case of waves on the surface of a fluid (Fig. 1) or in the case of a boundary layer of a viscous fluid on a plate when derivatives $\partial/\partial z$ in the perpendicular direction are present. The excitation force in this case is considered to be localized in all directions.

Let the zero initial condition be specified at the initial time:

$$u_i(x,0) = 0;$$

if the order of the system of equations is higher than one in time, then the corresponding derivatives are also set to zero. Thus, the solution obtained below corresponds to the excitation only by the source.

First, apply the Fourier transform with respect to the coordinate x to this system of equations, and then apply the Laplace transform with respect to time t. We denote the parameter of the Fourier transform by

k, and for a more convenient physical interpretation of the results obtained below, we use $\omega = is$ as the parameter of the Laplace transform rather than the standard parameter s. Then we obtain

$$\begin{aligned} P_{11}U_1 + P_{12}U_2 + \ldots + P_{1n}U_n &= \frac{f_1}{-\sqrt{2\pi}i(\omega - \omega_0)}, \\ P_{21}U_1 + P_{22}U_2 + \ldots + P_{2n}U_n &= \frac{f_2}{-\sqrt{2\pi}i(\omega - \omega_0)}, \\ \ldots\ldots\ldots\ldots & \\ P_{n1}U_1 + P_{n2}U_2 + \ldots + P_{nn}U_n &= \frac{f_n}{-\sqrt{2\pi}i(\omega - \omega_0)}, \end{aligned} \tag{3.1}$$

where $P_{ij} = P_{ij}(ik, -i\omega)$ and $U_i(k, \omega)$ are the transformed unknowns. If the original system is not purely one-dimensional, i.e., if it includes derivatives with respect to the other coordinates, then we assume that the differential problem in the other directions can be solved in the transformed variables (possibly not uniquely if there are more than one mode in the transverse directions).

For example, in the case of waves on a fluid surface (Fig. 1), it is required that the disturbances damp as $z \to \pm\infty$, which implies that the transformed unknowns for $k \in \mathbb{R}$ depend on z as $e^{-|k|z}$ as $z \to +\infty$ and as $e^{|k|z}$ as $z \to -\infty$. Satisfying the boundary conditions at $z = 0$ allows us to eliminate the variable z for the transformed variables U_i.

Thus, the transverse variables in (3.1) can be considered eliminated. However, P_{ij} is, generally speaking, not a polynomial function anymore—the presence of $|k|$ in the dependences on z generates a cut when isolating a single-valued branch $|k|$ along the straight line $\operatorname{Re} k = 0$, and, as will be seen below, this will lead to the emergence of a continuous spectrum in the solution.

The solution to the resulting inhomogeneous system of linear algebraic equations (3.1) can be written in the form of Cramer's formulas

$$U_j(k, \omega) = \frac{\mathcal{D}_j(k, \omega)}{\mathcal{D}(k, \omega)}, \tag{3.2}$$

where

$$\mathcal{D}(k, \omega) = \begin{vmatrix} P_{11}(ik, -i\omega) & P_{12}(ik, -i\omega) & \ldots & P_{1n}(ik, -i\omega) \\ P_{21}(ik, -i\omega) & P_{22}(ik, -i\omega) & \ldots & P_{2n}(ik, -i\omega) \\ \ldots & \ldots & \ldots & \ldots \\ P_{n1}(ik, -i\omega) & P_{n2}(ik, -i\omega) & \ldots & P_{nn}(ik, -i\omega) \end{vmatrix}$$

is the determinant of the system of equations and $\mathcal{D}_j$ are the determinants of the matrices with the columns replaced by the vector of the right-hand side. Note that the equation $\mathcal{D}(k, \omega) = 0$ specifies the dispersion equation of the problem; i.e., it relates the wave number with the frequency in the traveling waves $\sim e^{i(kx - \omega t)}$.

The original variables are obtained from the found transformed variables by applying the inverse Fourier transform and then the inverse Laplace transform:

$$u_i(x, t) = \frac{1}{(2\pi)^{3/2}} \int_\Gamma \left(\int_{-\infty}^{+\infty} U_j(k, \omega) e^{ikx} dk \right) e^{-i\omega t} d\omega. \tag{3.3}$$

The contours of integration are shown in Fig. 3, and the contour Γ lies above all the singularities of the integrands in the complex plane ω.

First, we calculate the inner integral with respect to k. Since the original system satisfies the causality principle, its traveling waves cannot grow arbitrarily fast, i.e., $M = \max_{k \in \mathbb{R}} \operatorname{Im} \omega(k) < \infty$, where $\omega(k)$ are solutions to the dispersion equation. In other words, there is a maximum of the increment of the traveling waves. This implies that for $\operatorname{Im} \omega > M$ the values of $k(\omega)$ cannot be real and are divided into two subsets $\operatorname{Im} k < 0$ and $\operatorname{Im} k > 0$. The internal integral in (3.3) contains singularities of two types. The singularities of the first type are the zeros of the denominator in (3.2), i.e. the solutions to the dispersion equation $k(\omega)$.

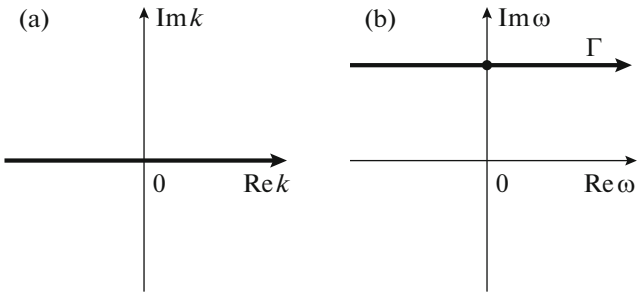

Fig. 3. Integration path for the inverse Fourier (a) and Laplace (b) transforms.

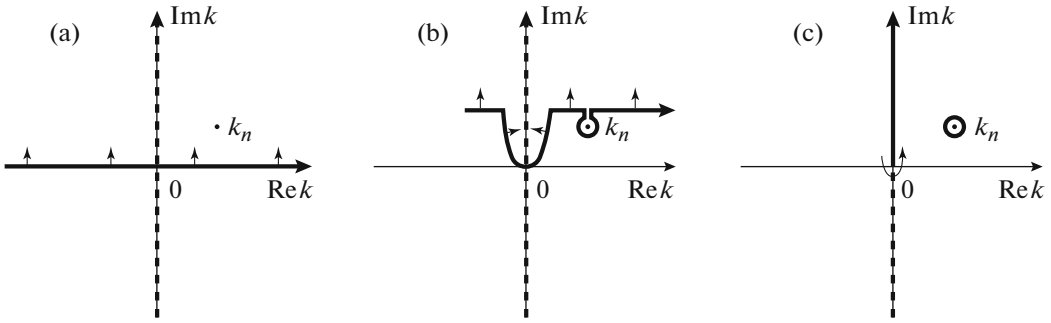

Fig. 4. Deformation of the integration path for the inverse Fourier transform for $x > 0$: original contour (a), deformation when going around a cut in the plane of k and of poles k_n (b), final contour consisting of integration along the cut and integration around poles (c). The bold solid line shows the integration contour, the dashed line shows the cut, and the dot shows the pole.

Since the value of the internal integral is calculated for $\operatorname{Im}\omega > M$, there are no such solutions on the real axis due to the above reasoning. The singularities of the second type are possible cuts of the complex function k appearing due to the non-one-dimensionality of the problem or for other reasons. Taking these remarks into account, for $x > 0$ the integration contour in the plane k can be deformed upwards as shown in Fig. 4, in which case the integrals along the cut and the integrals around the poles (3.2) (i.e., the spatial eigenmodes, which are calculated using the theory of residues) are singled out. The remainder of the integral tends to zero when deformed upwards since in the case $x > 0$, $e^{ikx} \to 0$ as $\operatorname{Im} k \to +\infty$. As a result, the internal integral in (3.3) for $\operatorname{Im}\omega > M$ is calculated in the form

$$U_j(x,\omega) = \int_{-\infty}^{+\infty} U_j(k,\omega)e^{ikx}dk = \sum_n a_j(\omega)e^{ik_n(\omega)x} + \int_0^{+\infty} b(k,\omega)e^{ikx}dk. \tag{3.4}$$

The first term expresses the contribution to the solution from the discrete spectrum—the solutions to the dispersion equation $k_n(\omega)$ lying for $\operatorname{Im}\omega > M$ in the upper half-plane $\operatorname{Im} k > 0$. The second term expresses the contribution to the solution from the continuous spectrum if it is present in the problem (i.e., if there is a cut of the plane k); here it is assumed that the cut of the plane k coincides with the imaginary axis; otherwise, the contribution is made by all cuts; e.g., in the problem of boundary layer disturbances there are two such cuts ([7], Subsections 7.1 and 7.3).

The solution for $x < 0$ is obtained similarly; in this case, the integration contour should be deformed downwards, and the solution contains the modes $k(\omega)$ lying for $\operatorname{Im}\omega > M$ in the lower half-plane $\operatorname{Im} k < 0$ and the parts of the continuous spectrum lying in the lower half-plane.

Next, we calculate the outer integral in (3.3). For this purpose, we deform the integration contour in the plane ω downwards. Then, the functions in (3.4) contain a single singularity—a pole in the form of the factor $1/(\omega - \omega_0)$. A path around it is shown in Fig. 5; the further deformation of the contour downwards in the complex plane ω lets the integral tend to zero, and the remaining integral around the pole is calculated using the residue theorem.

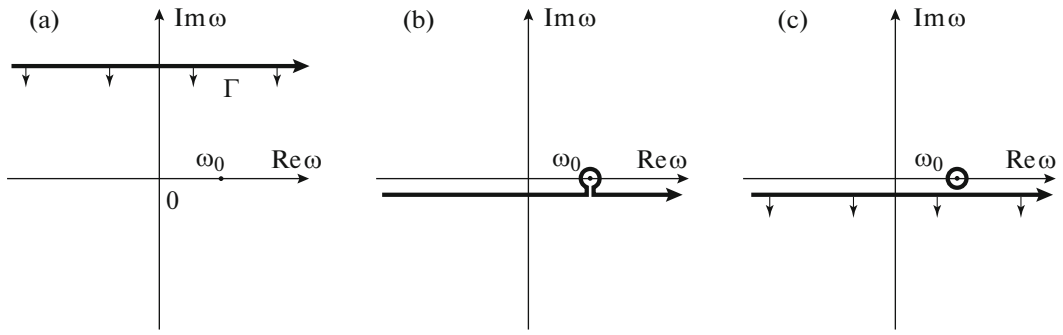

Fig. 5. Deformation of the integration path for the inverse Laplace transform: original contour (a), deformation when going around the pole (b), final contour consisting of integration around the pole; the integral along the remaining horizontal contour equals zero since it goes downwards to infinity (c). The contour of integration is shown by the thick solid line, and the pole, by the dot.

As a result, we obtain the following solution to the Cauchy problem for $t > 0$:

$$u_j(x,t) = \sum_n A_n(\omega_0) e^{i(k_n(\omega_0)x - \omega_0 t)} + \int_0^{+\infty} B(k,\omega_0) e^{i(kx-\omega_0 t)} dk, \tag{3.5}$$

where $A_n(\omega)$ and $B(\omega)$ are functions the exact form of which is not important for the further analysis.

Let us make several comments on the obtained solution. First, we note that the modes included in sum (3.5) for $x > 0$ correspond only to those values of $k_n(\omega_0)$ that are in the upper half-plane of k as $\operatorname{Im}\omega \to +\infty$, and for $x < 0$ they are in the lower half-plane of k. This gives a criterion for determining which waves move to the right and which to the left, since these waves are the ones that contribute to the exact solution to the problem of the source to the right and left of the introduced disturbance.

Secondly, the solution includes a continuous spectrum (if it is present in the problem, as discussed above): for $x > 0$ the solution includes only the part of it that lies in the upper half-plane; for $x < 0$, it includes the part that lies in the lower half-plane of k.

Thirdly, while solving the problem, we assumed that the number of discrete modes $k_n(\omega_0)$ does not change during the deformation of the Laplace contour and the integrand in the continuous spectrum does not contain singularities during the deformation. These conditions are violated if one of the discrete modes is absorbed by the continuous spectrum and disappears during the deformation of the Laplace contour, or, conversely, emerges from it; this case will be considered separately below.

Fourthly, the deformation of the integration contours, according to the Cauchy theorem, is possible only in finite-size regions; the possibility of deformation of the "tails" of the integration contours requires separate justification. Usually, such a possibility is ensured by a power-law decrease of the integrands in the tails, which is caused by the predominance of capillary and viscous effects in short-wave and high-frequency processes.

Finally, the problem statement itself can be modified. Rather than considering the disturbances propagating from a localized source for $x > 0$ and $x < 0$, we may investigate a semi-infinite problem in the domain $x > 0$ or $x < 0$ with given boundary conditions at $x = 0$ that generate disturbances. In this case, the application of the one-sided Fourier transform with respect to x and the Laplace transform with respect to t leads to a system similar in structure to (3.1), where the right-hand side is determined by the boundary conditions. The further deformation of the integration contours and the final solution have the same form (3.5) as in the source problem.

3.2. Physical Interpretation

From the exact solution to the Cauchy problem (3.5), we obtain the Briggs criterion: the contribution to the solution to the right and left of the source is given only by the modes that lie in the upper and lower planes of k, respectively, as $\operatorname{Im}\omega \to +\infty$. However, as $\operatorname{Im}\omega$ decreases, the location of the roots $k_n(\omega)$ can change, and they can intersect the real axis. In particular, for real values of the frequency, the location of the roots $k_n(\omega)$ can be completely different from that for large values of $\operatorname{Im}\omega$. Therefore, to determine the

true direction of wave motion, it is necessary to increase $\operatorname{Im}\omega$ and track in which half-plane each root remains.

This process may be looked at from another point of view. When introducing a disturbance with a real frequency ω_0, the waves scattered in different directions can be amplified with distance from the source due to instability. However, adding a positive increment $\operatorname{Im}\omega$ to the source is equivalent to an exponential amplification in time of the introduced disturbances. Whatever the spatial amplification of the diverging waves, it will be "outweighed" by a sufficiently fast exponential temporal amplification of the source, so that for sufficiently large $\operatorname{Im}\omega$, i.e., for a very fast temporal amplification of the disturbance in the source, the value of $\operatorname{Im}k$ will become a reliable indicator: exponentially decaying in space waves should diverge from the source with a very fast amplification, i.e., with $\operatorname{Im}k > 0$ for $x > 0$ and $\operatorname{Im}k < 0$ for $x < 0$.

3.3. Amplification and Non-Transparency

As shown earlier, for real values of the frequency, neither the phase nor the group velocity can be an indicator of the direction of wave propagation. Situations are possible such that $\operatorname{Im}k < 0$, i.e. the wave intensifies with distance in the positive direction of the axis x, but this intensification can be a consequence of either the spatial growth of the wave moving to the right (a consequence of instability) or the spatial attenuation of the wave moving to the left. In the "physical" language, the first situation is sometimes called wave amplification, and the second one is called non-transparency, i.e. the damping of the wave as it propagates to the left (see [18, 19], Subsection 63). The criterion obtained above allows us to unambiguously distinguish between these two cases: if $\operatorname{Im}k(\omega) > 0$ as $\operatorname{Im}\omega \to +\infty$, then such a wave corresponds to amplification, i.e. to the instability of the system. Otherwise, non-transparency takes place, i.e. the wave moves in the negative direction of the axis x and at the same time exponentially decays—the system resists its motion.

3.4. Relationship with Naïve Wave Direction Indicators

For small changes in frequency or wave number, their relationship is described by the so-called Gaster transformation ([7], Subsection 7.1.3, [20]), which is sometimes used when going from a temporal stability problem to a spatial one and vice versa near the neutral curve. Namely, let $k(\omega) = k_0$ for $\omega = \omega_0$. Adding a small change to the frequency $\omega = \omega_0 + i\delta$, $\delta > 0$, we have an expansion according to the Taylor formula:

$$k(\omega) = k(\omega_0) + \left.\frac{dk}{d\omega}\right|_{\omega=\omega_0}(\omega - \omega_0) + \ldots = k_0 + \left.\frac{dk}{d\omega}\right|_{\omega=\omega_0} i\delta + \ldots = k_0 + \frac{i}{g(\omega_0)}\operatorname{Im}\omega + \ldots . \tag{3.6}$$

Since $\operatorname{sign}\operatorname{Re}(1/g(\omega_0)) = \operatorname{sign}\operatorname{Re}g(\omega_0)$, the direction of the vertical displacement of $k(\omega)$ at low increment of $\operatorname{Im}\omega$ is given by the value of the group velocity $\operatorname{Re}d\omega/dk$. Thus, the group velocity shows the direction of the "initial" change of $\operatorname{Im}k$ at low increment of $\operatorname{Im}\omega$.

In the general case, the root $k(\omega)$ moving up or down with a small increase in $\operatorname{Im}\omega$ can turn around and go in the other direction (Fig. 6). In other words, the sign of the group velocity allows us to understand the behavior of the roots "in the first approximation," but in the general case it is unreliable.

Nevertheless, we prove that the group velocity can be correctly used to identify the direction of motion of a wave with $k \in \mathbb{R}$ if this wave is the fastest growing one. Let us assume that this is not the case, i.e., let there exist a real k_0 such that $\operatorname{Im}\omega(k_0)$ is the largest among all real k. A small increase in $\operatorname{Im}\omega$ will lead to a "false" direction of motion of $k(\omega)$, after which sooner or later a reversal will occur, and $k(\omega)$ will move to its "correct" half-plane. In this case, the next intersection of the real axis by k will inevitably occur (Fig. 6). That is, there is a $k_1 \in \mathbb{R}$ such that $\operatorname{Im}\omega(k_1) > \operatorname{Im}\omega(k_0)$, which refutes the initial assumption and proves the statement.

Thus, we have proved the correctness of using the sign $\operatorname{sign}\operatorname{Re}g$ of the group velocity as a criterion for determining the direction of wave motion for the most rapidly growing disturbance. However, in the general case of modes that are not the most amplified, this is not the case. As an example of such a situation, Fig. 7 shows the calculation of the behavior of solutions $k(\omega)$ to the dispersion equation (2.1) for $\operatorname{Re}\omega = 0.9$ and increasing $\operatorname{Im}\omega$. Pay attention to the root $k_s(\omega)$: for a small increment of $\operatorname{Im}\omega$, it moves downwards, i.e., its group velocity is negative, and this root should be attributed to the wave propagating to the left. However, with a further increase of $\operatorname{Im}\omega$, it turns around and moves upwards, i.e., it corresponds to a wave moving to the right.

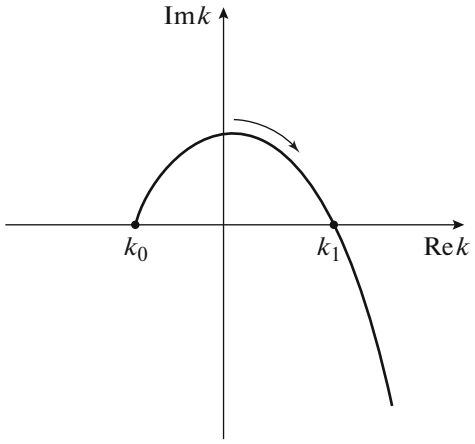

Fig. 6. To the proof of correctness of the group velocity sign for identifying the direction of motion of the most rapidly growing wave: example of the root $k(\omega)$ trajectory as $\operatorname{Im}\omega$ increases.

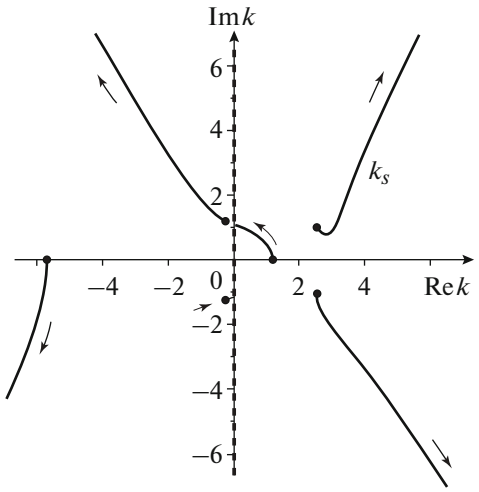

Fig. 7. Motion of the roots $k(\omega)$ to Eq. (2.1) for $\operatorname{Re}\omega = 0.9$ and $\operatorname{Im}\omega$ increasing from 0 (dots) to 10. The direction of root motion is shown by arrows. The dashed line depicts the continuous spectrum.

3.5. Continuous Spectrum and "Vanishing" Discrete Modes

The example shown in Fig. 7 is also interesting from another point of view. Namely, at $\omega = 0.9$ there are six roots of the dispersion equation (2.1) with parameters (2.4):

$$k = 1.194,\ 2.528 + 1.036i,\ 2.528 - 1.036i,\ -0.257 + 1.220i,\ -5.736,\ -0.257 - 1.220i.$$

We see that there are six spatial eigenmodes two of which are neutral. Their motion with increasing $\operatorname{Im}\omega$ is illustrated in Fig. 7. It can be seen that the neutral mode with $k = 1.194$ approaches the continuous spectrum, merges with it, and vanishes. The same happens with the mode corresponding to $k = -0.257 - 1.220i$. For large values of $\operatorname{Im}\omega$, there are only four eigenmodes $k(\omega)$.

The disappearance of a discrete mode formally does not allow the Briggs criterion to be applied to it since this mode does not exist in the k plane for large $\operatorname{Im}\omega$. To resolve this issue, we return to finding an exact solution to the Cauchy problem (3.5). When the Laplace contour moves downwards, the emergence of a new discrete mode from the continuous spectrum is accompanied by a singularity of the integral along the cut of the k plane since at this moment the integral in the second term of (3.5) passes through the pole. To remove this singularity, we can deform the integration contour in the k plane as shown in Fig. 8. In this case, a new discrete mode emerges from the continuous spectrum.

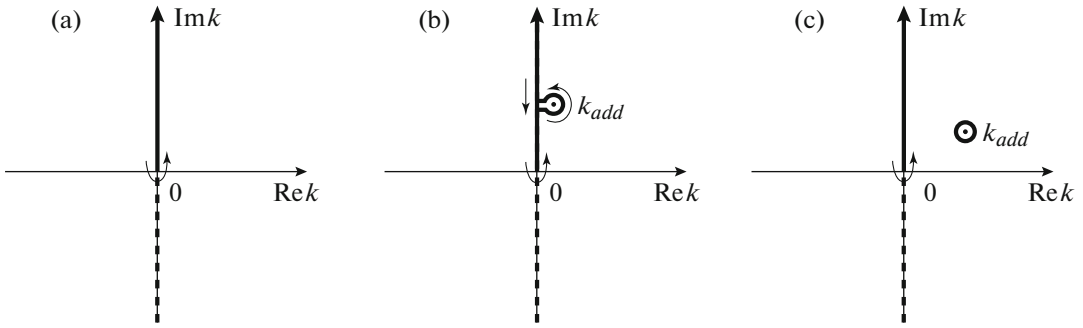

Fig. 8. Isolation of the new discrete mode emerging from the continuous spectrum as the Laplace contour goes down: original integral along the cut (a), emergence of a pole from the cut and its bypass (b), isolation of the pole bypass into a separate contour (c). The bold solid line shows the integration contour, the dashed line shows the cut, and the dot shows the pole.

Turning this picture in the opposite direction, i.e., with increasing $\operatorname{Im}\omega$, we obtain a generalization of the Briggs criterion for the direction of wave motion to the case of modes that vanish as $\operatorname{Im}\omega \to +\infty$: such modes move to the right if they disappear in the part of the continuous spectrum lying in the upper half-plane k, and they move to the left if they disappear in the lower half-plane.

3.6. Vanishing Modes in the Absence of a Continuous Spectrum

Consider this question from a different point of view. Since in the example (2.1) considered above the continuous spectrum was a consequence of an unbounded (with respect to z) region, consider an analog of this problem for the lower and upper layers of fluids of finite dimensions (Fig. 9). The dispersion equation in this case has the form (see [13], Chapter 8, Sections 12 and 13)

$$(\omega - Uk)^2 \coth(kL) + \varkappa\omega^2 \coth(kH) = (\varkappa - 1)k + k^3. \tag{3.7}$$

It is clear that as $L, H \to \infty$, Eq. (3.7) reduces to Eq. (2.1); however, for arbitrarily large but finite L and H, it has no cuts in the plane k. We prove that instead it has an additional discrete spectrum lying near the imaginary axis of k as $\operatorname{Im}\omega \to \infty$. In other words, the continuous spectrum "splits" into an additional countable subset of the discrete spectrum, as is the case in other problems of hydrodynamic stability [7].

To prove this statement, we consider the roots $k(\omega)$ of Eq. (3.7) for large $\operatorname{Im}\omega$. Denote $\omega = \omega_r + i\omega_i$ and consider the limit $\omega_i \to +\infty$. An analysis of the orders of magnitude of the quantities appearing in the dispersion equation shows that the limiting values of the roots fall into two types. The first roots do not lie near the imaginary axis and tend to infinity; for such roots lying in the right half-plane, we have

$$(\omega - Uk)^2 + \varkappa\omega^2 \sim k^3.$$

Hence $k \sim \omega^{2/3}$, and the further simplification yields

$$(1 + \varkappa)\omega^2 \sim k^3 \Rightarrow k \sim (-(1 + \varkappa)\omega_i^2)^{1/3},$$

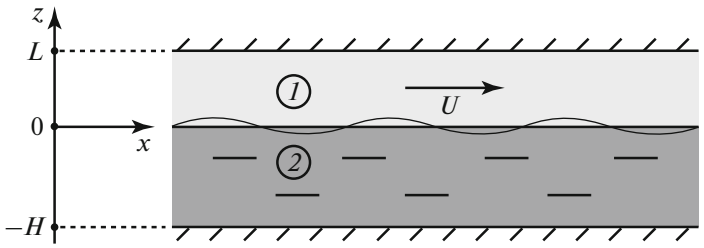

Fig. 9. Waves on the surface of heavy fluid of finite depth above which a layer of lighter fluid moves.

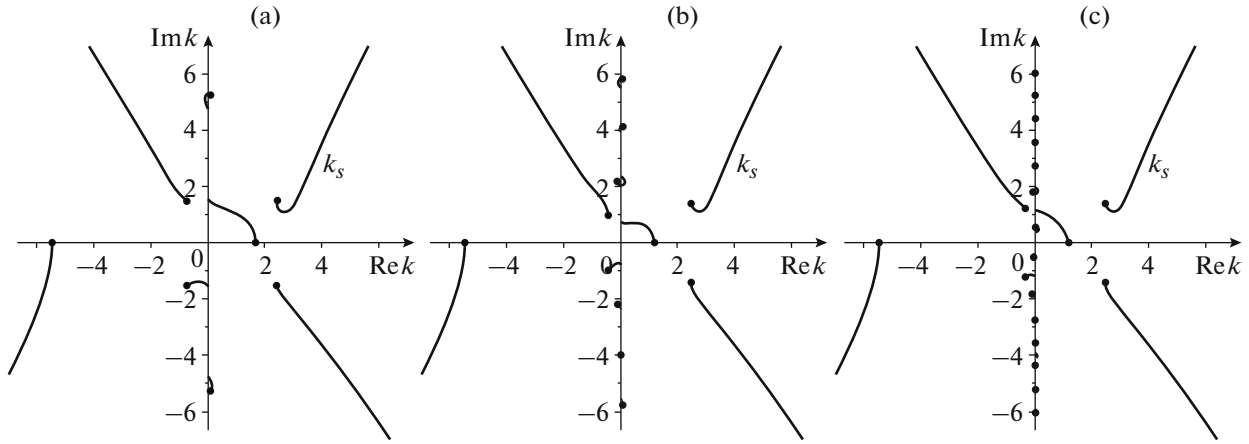

Fig. 10. Motion of the roots $k(\omega)$ to Eq. (2.1) for $\operatorname{Re}\omega = 0.9$ and $\operatorname{Im}\omega$ increasing from 0 (dots) to 10 at $L = H = 1$ (a), 2 (b), and 4 (c).

where two values of the cubic root lying in the region $\operatorname{Re} k > 0$ are taken. Similarly, two more roots in the region $\operatorname{Re} k < 0$ are obtained.

In addition to these four roots $k(\omega)$ (they are also present for $L = H = \infty$), there is another family of roots lying near the imaginary axis. Let $k = k_r + ik_i$. Assuming that $|k_r| \ll |k_i|$, we obtain

$$(\omega_i - Uk_i)^2 \cot(k_i L) + \varkappa\omega_i^2 \cot(k_i H) = (\varkappa - 1)k_i - k_i^3.$$

Reducing by ω_i^2, we obtain for k_i satisfying the condition $|k_i| \lesssim \omega_i^{2/3}$ the equation

$$\cot(k_i L) + \varkappa \cot(k_i H) = 0.$$

It has a countable number of roots; therefore, as $\omega_i \to +\infty$ the second family of roots consists of countable set lying near the imaginary axis.

The calculated location of the spectrum points for $L = H = 1$ and $\omega = 0.9$ and the trajectories of the roots $k(\omega)$ as $\operatorname{Im}\omega$ increases are shown in Fig. 10a. As can be seen, the vanishing modes are preserved, but as $\operatorname{Im}\omega \to \infty$ they tend to constant values located on the imaginary axis, i.e. where the continuous spectrum is located when $L, H = \infty$. As L and H increase (see Fig. 10b) this behavior is preserved, and the imaginary axis of k is saturated with discrete spectrum modes, which, as $L, H \to \infty$, fill it completely thus turning into a continuous spectrum.

Note that, unlike Eq. (3.7), where discrete modes tend to constants lying on the imaginary axis as $\operatorname{Im}\omega \to \infty$, the vanishing modes of Eq. (2.1) actually vanish—they pass to another, nonphysical, sheet of the Riemann surface of the function $|k|$, cease to satisfy the damping condition as $|z| \to \infty$, and do not remain near the imaginary axis in any sense. Thus, the behavior of the roots of Eqs. (3.7) and (2.1) near the imaginary axis is fundamentally different despite the fact that Eq. (2.1) is obtained from Eq. (3.7) by taking the limit. At the same time, the solution to the Cauchy problem on the propagation of disturbances from a source in the unbounded case is obtained by passing to the limit in the bounded problem due to the presence of a continuous spectrum in the unbounded problem. This apparent paradox is explained by the fact that the modes of the continuous spectrum in the unbounded problem are not modes in the true sense—they do not individually satisfy the damping condition at infinity; this condition is satisfied only by their superposition, i.e., during integration. At the same time, the modes of the discretized continuous spectrum are "real" modes in the bounded problem since they are not required to damp with distance from the interface but are only required to be equal to zero at a distant wall.

4. APPLICATION TO THE PROBLEM OF HYDRODYNAMIC STABILITY

Thus, using the wind model above a fluid layer, we have shown that, firstly, the phase and group velocities can erroneously predict the direction of wave motion. Secondly, the application of the physically justified Briggs criterion, which consists of calculating $\lim_{\operatorname{Im}\omega\to+\infty} \operatorname{sign} \operatorname{Im} k(\omega)$, can be impossible due to the

absorption of the discrete mode under consideration by the continuous spectrum at large values of $\mathrm{Im}\,\omega$ and, and consequently, due to the nonexistence of the limit. At the same time, in the considered rather simple model, which allows an analytical study of the function $k(\omega)$, these issues can be resolved based on physical considerations. This section is devoted to a more complex case of the problem of hydrodynamic stability of a submerged fluid jet, where the same effects are observed but an analytical study or simple physical considerations are no longer possible.

4.1. Statement of the Submerged Jet Problem and a Method for Its Numerical Solution

Let us consider a round submerged jet with the velocity profile shown in dimensionless form in Fig. 11 (the maximum velocity and the jet radius are taken as the non-dimensionalization scales). This profile corresponds to that obtained in the experimental facility [21, 22] at a distance from the nozzle outlet section $z/D = 0.5$, where D is the jet diameter. The Reynolds number corresponding to this profile is $\mathrm{Re} = 6122$. The experimentally measured velocity distribution was approximated by a smooth function, which is used in subsequent calculations. This velocity profile has three inflection points (Fig. 11) and three generalized inflection points (they responsible for instability in axisymmetric flows [23]), which generate two instability modes. The instability is convective in nature [24].

To calculate the spatial spectrum in the plane-parallel approximation, the Navier–Stokes equations system is considered; this system was linearized around a steady flow with the velocity profile $\mathbf{U} = (0,0,U(r))$

$$\frac{\partial \mathbf{u}'}{\partial t} + \mathbf{U}\cdot\nabla\mathbf{u}' + \mathbf{u}'\cdot\nabla\mathbf{U} = -\nabla p' + \frac{1}{\mathrm{Re}}\Delta\mathbf{u}',$$

$$\nabla\mathbf{u}' = 0,$$

where $\mathbf{u}'$, p' are the disturbances of the velocity and pressure, and its axisymmetric solutions have in the cylindrical system of coordinates the form

$$\begin{pmatrix} u'(r,\theta,z) \\ v'(r,\theta,z) \\ w'(r,\theta,z) \\ p'(r,\theta,z) \end{pmatrix} = e^{i(kz-\omega t)} \begin{pmatrix} \tilde{u}(r) \\ \tilde{v}(r) \\ \tilde{w}(r) \\ \tilde{p}(r) \end{pmatrix}.$$

The eigenmodes must satisfy the zero boundary conditions for the velocity disturbance components as $r \to +\infty$ and the kinematic conditions [23] at $r = 0$. In the numerical solution, the external zero boundary condition is set at a sufficiently large value of $r = R_{\mathrm{out}}$, which is selected based on an analysis of the convergence of the solution with increasing R_{out}. The calculations below are given for $R_{\mathrm{out}} = 10$; this value is

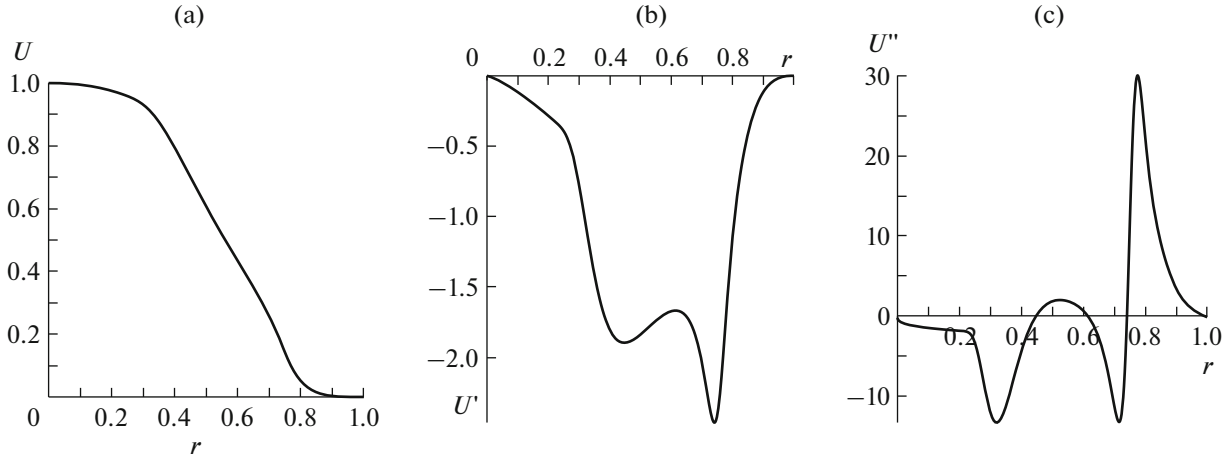

Fig. 11. Jet velocity profile and its derivatives $U(r)$ (a), $U'(r)$ (b), and $U''(r)$ (c).

sufficient for the convergence of the considered part of the discrete spectrum. The spatial eigenvalue problem was solved by the spectral method described in detail in [4, 6].

4.2. The Behavior of Spectrum as Im ω Increases

In Fig. 12, the calculated spatial spectrum at $\omega = 1$ is shown by dots, and the motion of modes is shown by lines for $\omega = 1 + i\omega_i$, $0 \leqslant \omega_i \leqslant 100$. Several families of modes can be distinguished in the spectrum. First, the modes lying near the imaginary axis k correspond to the continuous spectrum, which was discretized due to finite R_{out}. As R_{out} increases, they fill the imaginary axis and in the limit they fill it completely. The second family—the closely spaced modes of the discrete spectrum in the first quarter of the complex plane k—correspond to short-wave WKB oscillations of the disturbance amplitude localized between the center and the edge of the jet. These modes are similar to S-modes in near-wall flows. The third family consists of the "ordinary" modes of the discrete spectrum of which five are present in the shown section of the plane k. Four of them—k_{d1}, k_{d2}, k_{d3}, and k_{d4}—correspond to waves moving downstream—at $\omega \in \mathbb{R}$ two of them (k_{d1}, k_{d2}) are growing instability modes, and (k_{d3}, k_{d4}) are two decaying modes. The fifth mode k_u corresponds to a decaying wave moving upstream.

Note that the discrete mode k_u moving upstream is incorrectly recognized as moving downstream by the sign of both the group and the phase velocities. Namely, $\operatorname{Im} k$ increases with increasing $\operatorname{Im} \omega$; therefore, we have $\operatorname{Re} g(k) > 0$ due to expansion (3.6). Furthermore, since this mode lies in the fourth quadrant of the plane k at $\omega \in \mathbb{R}$, its phase velocity satisfies $\operatorname{Re} c(k) > 0$. Therefore, both naïve indicators give a direction of motion in the positive direction of the axis x, while the generalized Briggs criterion gives the opposite direction.

In addition, this mode, like the two downstream modes k_{d3} and k_{d4}, is absorbed by the continuous spectrum and disappears as $\operatorname{Im} \omega$ increases. Thus, it would be impossible to determine the direction of motion of these waves without the generalization of the Briggs criterion obtained in this paper.

Note that the analogs of the mode k_u, as well as other modes moving upstream, were correctly rejected as "non-physical" when analyzing wall flows in [10, 11]. However, there are no formal reasons to separate them from the instability modes k_{d1} and k_{d2}: these three modes have the same sign of the phase and group velocities and are located in the same quarter of the plane. Moreover, the analogs of the mode k_u are in

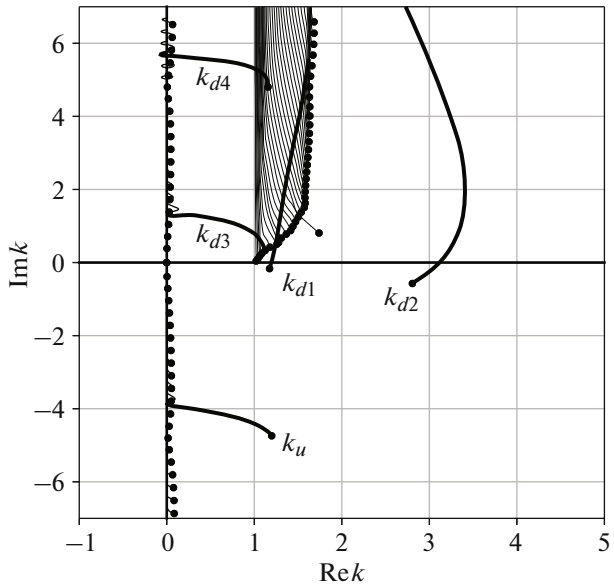

Fig. 12. Spatial spectrum $k(\omega)$ of the submerged jet for $\omega = 1 + i\omega_i$. Dots show the spectrum for $\omega_i = 0$, and the curves show the spectrum motion as ω_i increases. Thin lines show the motion of discrete WKB modes, bold lines show the motion of "ordinary" discrete modes, and ordinary lines show the motion of discrete representation of the continuous spectrum near the imaginary axis.

fact physical, but they propagate upstream and should have been taken into account if the problem of disturbance development were studied in the opposite direction (upstream). As can be seen from the results obtained above, there is no "simple" way other than generalizing the Briggs criterion to reasonably identify the direction of motion of the mode k_u and not include it in the set of modes moving downstream.

4.3. The Case of no Continuous Spectrum: Flow in a Pipe

Let us consider, similarly to Subsection 3.6, the situation when the boundary no-slip condition is set at $r = 1$, which is equivalent to the value $R_{\text{out}} = 1$. This can be physically interpreted as the flow of a jet into a pipe and its further motion in it with the velocity profile being preserved for a long distance; this can be considered justified due to the sufficiently large Reynolds number.

The result of the spectrum calculation in this case is shown in Fig. 13. Qualitatively, it corresponds to the structure of the spectrum of an unbounded jet (Fig. 12) with the exception that there is no continuous spectrum. The modes in the jet that are absorbed by the continuous spectrum, approach the imaginary axis in the case of a pipe, and as $\operatorname{Im}\omega \to +\infty$ they tend to fixed points on the imaginary axis, while remaining discrete modes. Thus, the behavior of the modes in the transition from an unbounded to a bounded problem is qualitatively similar to the case considered in Subsection 3.6.

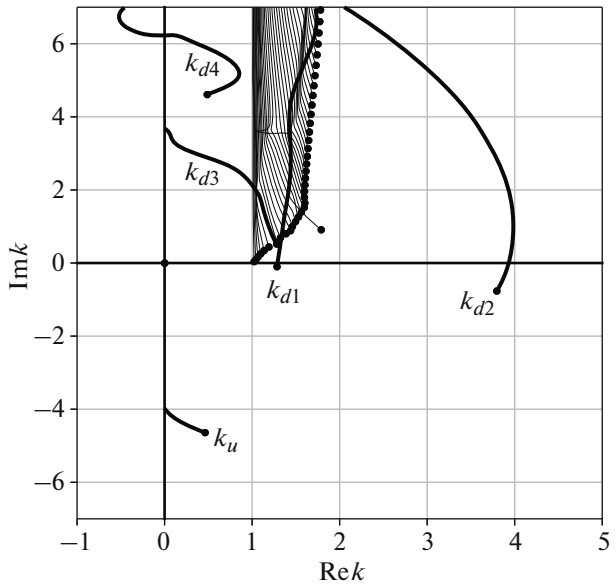

Fig. 13. Spatial spectrum $k(\omega)$ of the submerged jet enclosed in a pipe for $\omega = 1 + i\omega_i$. Dots show the spectrum for $\omega_i = 0$, and the curves show the spectrum motion as ω_i increases. Thin lines show the motion of discrete WKB modes and bold lines show the motion of "ordinary" discrete modes.

As in the jet, the direction of motion of the mode k_u is incorrectly identified by both the phase and group velocities. The Briggs criterion obviously gives the correct result, since the mode in the limit $\operatorname{Im}\omega \to +\infty$ remains within the region $\operatorname{Im} k < 0$.

5. CONCLUSIONS

The paper examines the direction of spatial propagation of a wave described by a complex-valued function $k(\omega)$, where ω is the frequency and k is the wave number. It is demonstrated that phase velocity cannot serve as an indicator of the direction of wave motion. It is proved that the group velocity, which is used in many studies as such an indicator, is also unreliable with the exception of the fastest growing wave.

To correctly identify the direction of wave motion, it is necessary to use the physically justified Briggs criterion, which follows from the principle of causality; namely, sign $\operatorname{Im} k(\omega)$ as $\operatorname{Im}\omega \to +\infty$. However, in this case, situations of discrete modes that vanish at large values of $\operatorname{Im}\omega$ due to their absorption by the continuous spectrum are possible. An example of a problem of waves on a fluid surface is discussed, in which such a situation is analyzed analytically. In this paper, the Briggs criterion is extended to such a case in a general form: the vanishing wave moves to the right if it is absorbed by the continuous spectrum lying in the region $\operatorname{Im} k > 0$, and it moves to the left otherwise.

An example of the problem of the stability of a submerged jet is demonstrated in which a disappearing mode arises accompanied simultaneously by a false identification of its direction of propagation by both phase and group velocities. The true direction of motion of such a wave is determined using the generalization of the Briggs criterion obtained in this work.

ACKNOWLEDGMENTS

I am grateful to D.A. Ashurov for calculating the spectrum of a submerged jet and to N.V. Nikitin for useful remarks.

FUNDING

This work was supported by the Russian Science Foundation, project no. 19-71-30012.

CONFLICT OF INTEREST

The author declares that he has no conflicts of interest.

REFERENCES

1. R. Hersh, "Boundary conditions for equations of evolution," Arch. Rat. Mech. Anal. **16** (4), 243–264 (1964).
2. P. Andersson, M. Berggren, and D. S. Henningson, "Optimal disturbances and bypass transition in boundary layers," Phys. Fluids **11**, 134–150 (1999).
3. E. Reshotko and A. Tumin, "Spatial theory of optimal disturbances in a circular pipe flow," Phys. Fluids **13**, 991–996 (2001).
4. O. O. Ivanov, D. A. Ashurov, L. R. Gareev, and V. V. Vedeneev, "Non-modal perturbation growth in a laminar jet: An experimental study," J. Fluid Mech. **963**, A8 (2023).
5. D. A. Ashurov and N. V. Nikitin, "Development of stationary disturbances in a spatially developing jet," Fluid Dyn. **59** (4), 723–731 (2024).
6. D. A. Ashurov, "Optimal disturbances in round submerged jets," Phys. Fluids **36**, 104118 (2024).
7. P. L. Schmid and D. S. Henningson, *Stability and Transition in Shear Flows* (Springer, 2001).
8. A. Towne and T. Colonius, "One-way spatial integration of hyperbolic equations," J. Comp. Phys. **300**, 844–861 (2015).
9. A. Towne, G. Rigas, O. Kamal, E. Pickering, and T. Colonius, "Efficient global resolvent analysis via the one-way Navier–Stokes equations," J. Fluid Mech. **948**, A9, (2022).
10. G. V. Zasko, A. V. Boiko, K. V. Demyanko, and Y. M. Nechepurenko, "Simulating the propagation of boundary-layer disturbances by solving boundary-value and initial-value problems," Russ. J. Numer. Anal. Math. Model. **39** (1), 47–59 (2024).
11. A. V. Boiko, K. V. Demyanko, G. V. Zasko, and Yu. M. Nechepurenko, "On the parabolization of equations for the propagation of small disturbances in two-dimensional boundary layers," Thermophys. Aeromech. **31** (3), 393–410 (2024).
12. V. V. Vedeneev, *Mathematical Theory of Stability of Plane-Parallel Flows and the Development of Turbulence* (Intellekt, Dolgoprudnyi, 2016) [in Russian].
13. N. E. Kochin, I. A. Kibel, and N. V. Roze, *Theoretical Hydromechanics,* Part 1 (Fizmatgiz, Moscow, 1963) [in Russian].
14. L. D. Landau and E. M. Lifshitz, *Fluid Mechanics,* 2nd ed. (Nauka, Moscow, 1986; Pergamon, Oxford, 1987).
15. I. G. Petrovskii, "On the Cauchy problem for systems of linear partial differential equations in the domain of nonalaytic functions," Bull. Mosk. Univ., Sect. A. Mat. Mekh. **1** (7), 16 (1938).
16. R. J. Briggs, *Electron-Stream Interaction with Plasmas* (MIT Press, 1964).
17. D. E. Ashpis and E. Reshotko, "The vibrating ribbon problem revisited," J. Fluid Mech. **213**, 531–547 (1990).

18. A. I. Akhiezer and R. V. Polovin, "Criteria for wave growth," Phys.–Usp. **14** (3), 278–285 (1971).
19. E. M. Lifshitz and L. P. Pitaevskii, *Physical Kinetics* (Nauka, Moscow, 1979; Pergamon, Oxford, 1981).
20. M. Gaster, "A note on the relation between temporally-increasing and spatially-increasing disturbances in hydrodynamic stability," J. Fluid Mech. **14** (2), 222–224 (1962).
21. J. Zayko, S. Teplovodskii, A. Chicherina, V. Vedeneev, and A. Reshmin, "Formation of free round jets with long laminar regions at large Reynolds numbers," Phys. Fluids **30**, 043603 (2018).
22. I. R. Gareev, J. S. Zayko, A. D. Chicherina, V. V. Trifonov, A. I. Reshmin, and V. V. Vedeneev, "Experimental validation of inviscid linear stability theory applied to an axisymmetric jet," J. Fluid Mech. **934**, A3 (2022).
23. G. K. Batchelor and A. E. Gill, "Analysis of the stability of axisymmetric jets," J. Fluid Mech. **14** (4), 529–551 (1962).
24. V. Vedeneev and J. Zayko, "On absolute instability of free jets," J. Phys. Conf. Ser. **1129**, 012037 (2018).

Translated by A. Klimontovich